arXiv:1704.03065v1 [cs.NI] 10 Apr 2017

MoMo: a group mobility model for future generation mobile wireless networks

Luca De Nardis, *Member, IEEE,* and Maria-Gabriella Di Benedetto, *Fellow, IEEE*

Abstract—Existing group mobility models were not designed to meet the requirements typical of current and future short distance wireless networks scenarios, that need, in particular, accurate, up-to-date information on the position of each node in the network, combined with a simple and flexible approach to mobility modeling.
A new model for group mobility in wireless networks, named MoMo, is proposed in this paper, based on the combination of a memory-based individual mobility model with a flexible group behavior model. MoMo is capable of accurately describing all mobility scenarios, from individual mobility, in which nodes move independently one from the other, to tight group mobility, where mobility patterns of different nodes are strictly correlated.
A new set of intrinsic properties of a mobility model is proposed and adopted in the analysis and comparison of MoMo with existing models. Results show that MoMo leads to accurate, robust and flexible modeling of mobility of groups of nodes, making it suitable for the wide range of network scenarios expected to characterize the deployment of 5G networks.

Index Terms—Mobility modeling, group mobility, 5G.

1 Introduction

THE evolution of wireless mobile networks in the last 20 years, moving from GSM/GPRS, through UMTS/HSDPA, to LTE and, as of lately, proposals for 5G systems to come, shows two dominating trends in network design. A first trend is an increase in physical layer flexibility, in order to meet user requirements and provide higher robustness to channel impairments as channel bandwidth increases. A physical layer parameter clearly highlighting this trend is the Transmission Time Interval (TTI), defined as the shortest time interval over which link configuration can be adjusted: Figure 1 shows TTI across four generations of wireless standards, moving from 20 ms in GSM/Edge [1], to about 0.15 ms as recently proposed for 5G systems [2].
A second trend is the increase in spatial density of wireless devices, from 1000 devices per square kilometer in GSM, to the millions of devices per square kilometer envisioned for 5G networks [3], leading to a corresponding decrease in the average distance between transmitter and receiver, from hundreds of meters in GSM networks to a few meters or below in 5G systems. The progressive increase in device density across generations led to major paradigm shifts in physical layer and network layer design. At physical layer, signal processing techniques were developed in order to cope with increasingly challenging throughput and latency requirements of dense deployments. In particular, in 3G and 4G systems, beamforming was introduced, based on Multiple Input Multiple Output (MIMO). Beamforming is expected to play a key role in 5G networks with the deployment of Massive MIMO [4]. As a matter of fact, beamforming techniques rely on the capability of determining the relative position of transmitter vs. receiver in order to determine the beam direction, and react swiftly to position changes [5]. At network layer, network topology moved from a purely centralized configuration, typical of 2G and 3G systems, to a mixed nature, combining infrastructure elements with Device-To-Device (D2D) connectivity as proposed in LTE [6]. 5G is expected to exacerbate the above trend, leading to scenarios where most of the traffic is transferred on D2D, short distance links typically activated among devices that share similar mobility patterns, with connectivity heavily influenced by device mobility due to the limited radio coverage area [7]. Application scenarios for short range wireless technologies, where small scale movements can dramatically change network topology, have emerged [8], that foresee small groups of people moving in a coordinated manner, while keeping a significant degree of independence in their individual mobility patterns. Examples include:

- search and rescue operations in response to emergency

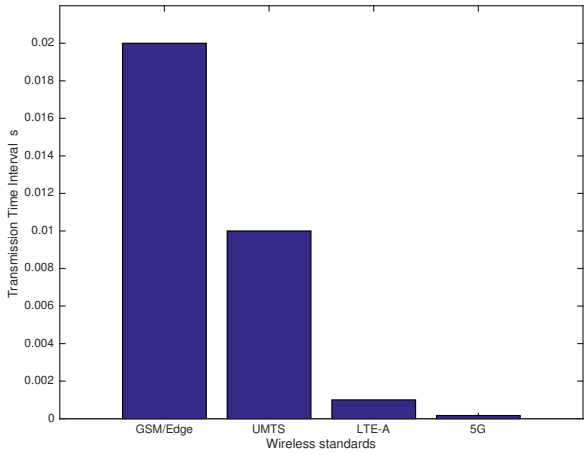

Fig. 1. Evolution of Transmission Time Interval across generations of cellular networks.

- *Both authors are with the Department of Information engineering, Electronics and Telecommunications at Sapienza University of Rome.*

Manuscript received April 19, 2005; revised August 26, 2015.

calls or disasters, in which, according to best practice rules, operators must work in groups of at least two while keeping visual or voice contact [9];
- tactical and security teams, with on-demand formation, merging and splitting of groups [10].

The above analysis indicates that, as wireless mobile networks evolve, wireless links must be adjusted more frequently and cover shorter and shorter distances, among devices with similar mobility patterns. Reliable performance evaluation requires thus the capability of determining with high accuracy and high refresh rate the position of wireless devices, calling for the definition of a mobility model capable of providing an accurate description of individual movement patterns and a flexible definition of relationship between nodes, allowing for seamlessly switching between individual node mobility and group mobility and viceversa, and enabling thus dynamic group fusions and partitions.
Accurate and flexible modeling of mobility for wireless mobile networks is a difficult task. As a consequence, models proposed in the past focused on specific mobility scenarios, with a dichotomy, in particular, for individual vs. group mobility models. Section 2 and Section 3 provide a review of most relevant individual vs. group mobility models; [11], [12] offer extensive surveys.
Focusing on group mobility models, the most popular one is by far the Reference Point Group Mobility (RPGM) model [13], widely used for performance evaluation of protocols for wireless mobile networks. RPGM was, however, originally proposed for scenarios where a rough description of node mobility is sufficient (e.g. in modeling mobility of cellular subscribers or users in ad-hoc networks over movement spans of hundreds or thousands of meters), and it is not able to provide the exact position of all nodes at all times, as required by mobility scenarios identified above. More recently, the DynaMo model was proposed in [14] to model the group mobility emerging from relationships between players during a soccer match. The suitability of the model for application scenarios typical of short distance mobile wireless networks was however not assessed in [14], and the impact of the model on network topology was not analyzed.
Other group mobility models were proposed as well, but in most cases they failed to gain support in the research community, either due to limited accuracy in modeling group relations or to excessive complexity in their implementation and tuning. A critical analysis of group mobility models is carried out in Section 3.
This paper addresses the issue of accurate and flexible mobility modeling in short distance wireless networks by proposing the MoMo model. MoMo combines the grouping approach proposed in [14] with an individual mobility mode selected so to satisfy the following requirements: a) guarantee that upper bounds on linear and angular speed characterizing the specific application scenario are met at all times by all nodes in the network, b) be able to provide the position of each node in the network at all times, c) manage seamlessly group formation, disbanding, merging and splitting. This work also proposes a set of properties a mobility model must show in order to properly model mobility in short distance wireless networks; they are 1) accuracy in modeling the desired mobility behavior, 2) robustness to variations of the input parameters, and 3) flexibility in dynamic mobility scenarios.
MoMo is compared against both individual and group mobility models, by means of computer simulation, using performance indicators related the above properties and to the impact on network topology and logical connectivity, as suggested in [15], [16].
The paper is organized as follows. Section 2 carries out a review of existing individual mobility models in order to identify a suitable candidate to be adopted in the MoMo model. Section 3 provides a critical analysis of existing group mobility models. Section 4 describes the MoMo model and introduces model parameters; Section 5 defines the proposed set of properties a mobility model should show, and the corresponding performance indicators. Section 6 presents simulation results related to the comparison of MoMo with existing models, and to the analysis of the impact of MoMo model parameters on the generated mobility patterns. Finally, Section 7 draws conclusions.

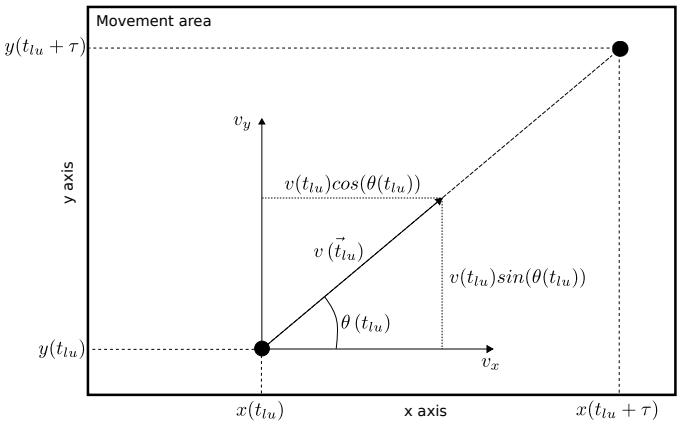

Fig. 2. Evaluation of position at time $t_{lu}+\tau$ as a function of speed vector updated at time t_{lu}.

2 Individual mobility models

Individual mobility models determine the pattern of each node by varying its speed vector, defined at generic time t as: $\vec{v(t)} = |v(t)|e^{j\theta(t)}$, where $|v(t)|$ is the speed absolute value and $\theta(t)$ is the direction of movement, defined as the angle between the x axis and the speed vector in the selected coordinate system. The position of a node can be obtained at any time τ between two updates of $\vec{v}$ as follows:

$$\begin{cases} x(t_{lu}+\tau) = x(t_{lu}) + v(t_{lu})\cos(\theta(t_{lu}))\tau \\ y(t_{lu}+\tau) = y(t_{lu}) + v(t_{lu})\sin(\theta(t_{lu}))\tau, \end{cases} \quad (1)$$

where t_{lu} is the time instant at which the speed vector was last updated, as shown in Figure 2. Models can be divided in two families, based on the way v and θ are selected and updated: *memoryless* vs. *memory-based* models.

2.1 Memoryless mobility models

In memoryless models the new values of speed and direction selected at each update are independent of current

and previous values. Well known models belonging to this family are:

- the *Random Walk* model, also referred to as Brownian model, that is one of the most widely used models in the simulation of wireless networks of mobile nodes [17]. The model was broadly used in the analysis of cellular networks, in order to determine the impact of mobility on network performance. Statistical models for reference mobility-related parameters, such as average cell crossing time, average channel holding time, and average number of handovers, were developed based on the assumption of a Random Walk user mobility model [17]. The model has also been used in mobile ad-hoc networks, for determining the performance of routing protocols in presence of node mobility [18].
In the Random Walk model, a node selects from time to time its speed and direction according to a uniform distribution. Depending on the selected flavor of the model, the selection of a new speed and direction is triggered by either of the following events:
  - A timer set to a predefined update period T expires [19];
  - The node covers a predefined distance D [11].
- the model proposed by Ko and Vaidya in [20] in order to evaluate the performance of the Location Aided Routing protocol. In this model, a node selects the direction at the beginning of simulation and keeps it constant. The node also selects its speed v within a predefined interval, and a distance d to be covered with the actual speed, selected according to an exponential distribution. After covering the distance, new values are selected for v and d. If the node hits a boundary of the simulation area, it is perfectly reflected within the area. The model was proposed as a simple solution to introduce mobility in network simulations, with no claims for specific advantages over other mobility models.
- the *Random Waypoint* model, originally proposed in [21]; the model is similar to the Random Walk model, the main difference being that the trajectory of a node is determined in this case by a sequence of destination points to reach. When a node reaches a destination point it pauses for a random time, and then moves towards the next destination point with a new random speed.
In the Random Waypoint model the time between two updates is inversely proportional to the selected speed. As a consequence, a node selecting a low speed spends a relatively large time moving towards the selected destination. It has been observed that this characteristic leads to large variations in the average number of neighbors (that is nodes within a given distance) seen by each node, especially on the short term [11]. Variations of this model have been proposed to address this issue, such as the Random Direction model, that forces the node to move at constant speed and keep the same direction until it reaches a boundary of the simulation area when, after a predefined pause time, a new random direction is selected according to a uniform distribution [22].

All memoryless models share the issue of potentially causing sharp turns and steep variations in speed when a new speed vector is selected, making it impossible to meet upper bounds on linear and angular speed, and leading to unrealistic mobility patterns.

2.2 Memory-based models

Memory-based models lead to more realistic patterns by introducing a memory effect in the selection of speed and direction. Well known models that adopt this approach are the following:

- the *Inertia* mobility model, proposed in [23], in which at each position update, new values for v and θ are selected with probability ρ, while the current set is kept with probability $1-\rho$. The ρ parameter models an inertia that tends to keep the node on the current trajectory: the higher the value of ρ, the lower the probability of selecting a new speed vector. For $\rho = 0$ the Inertia model falls back to the previously described Random Walk model.
- the *Gauss-Markov* model, proposed in [24], in which the component v_i of the speed vector along direction i (with $i \in [x, y]$ in a two-dimensional space) at time t is the outcome of a Gauss-Markov random process $v_i(t)$, that is a stationary Gaussian process characterized by the following autocorrelation function:

$$\phi_{v_i}(\tau) = E\left[v_i(t)\, v_i(t+\tau)\right] = \sigma_i^2 e^{-\beta|\tau|} + \mu_i^2 \qquad (2)$$

where σ_i^2 and μ_i are the variance and the mean of $v_i(t)$, respectively, and parameter $\beta \geq 0$ introduces a memory effect in the process. The mobility patterns generated by this model are governed by properly setting the β parameter.
- the *Boundless* mobility model, proposed in [25], taking its name from the idea of mapping a bi-dimensional simulation area on the surface of a three-dimensional torus: a node that reaches an edge of the area disappears, and reappears instantaneously on a point on the opposite edge, while keeping the same speed vector. The algorithm for speed and direction update proposed in [25], however, can be adopted within a traditional bounded movement area as well. In the Boundless model the speed vector is updated every T seconds according to the following equations:

$$\begin{cases} v(t+T) = \min\left(\max\left(v(t) + \Delta v, 0\right), v_{max}\right) \\ \theta(t+T) = \theta(t) + \Delta\theta, \end{cases} \qquad (3)$$

where:
  - v_{max} is the maximum speed;
  - Δv is the speed variation, uniformly selected at every update time in the interval $[-a_{max}T, a_{max}T]$, where a_{max} is the maximum linear acceleration allowed for a node, measured in m/s^2;
  - $\Delta\theta$ is the direction variation, uniformly selected at every update time in the interval $[-\gamma_{max}T, \gamma_{max}T]$, where γ_{max} is the maximum rotation speed allowed for a node, measured in rad/s.

3 Group mobility models

Group mobility models proposed in the literature can be classified in two families: reference-based models vs. behavioral models. In reference-based models, nodes belonging to the same group have their position determined as a deviation from a common reference, for example position or speed. Behavioral models define the rules that nodes obey in selecting their speed and direction; in these models groups naturally emerge when multiple nodes share same rules, and generate thus similar mobility patterns.

3.1 Reference-based models

The Exponential Correlated Random (ECR) mobility model, proposed in [26], was one of the first models taking into account correlation among different nodes. In the ECR model, a group is considered as a single entity: the model does not allow thus to describe the movement pattern of individual nodes in a group, except for the special case of a single node.

The Reference Point Group Mobility (RPGM) model was designed in order to overcome the limitations of the ECR model, by allowing the description of group as well as individual node mobility within a group [13]. The model defines a logical reference point for each group, whose movement is followed by all nodes in the group. The path followed by the reference point defines the entire group mobility behavior, including position, speed, direction and acceleration. An alternative solution for the definition of the reference path is to elect one of the nodes in each group as its leader, and to use the position of such node as the reference point for other nodes in the group, referred to as standard nodes.

The group trajectory is determined by providing a path for the group leader, and by refreshing the position of standard nodes every Δt seconds, randomly placing them within a distance d_{max} from the current position of the leader at each refresh. In [13] the path was defined using the Random Waypoint model described in Section 2.

Several variations of the RPGM model were proposed, in order to describe specific mobility scenarios, as for example the Pursue, Nomadic Community and Column mobility models, introduced in [27]. The Structured Group Mobility Model [28] extended the RPGM model by allowing the use of different distributions for different nodes, in the generation of relative distance and angle with respect to the reference point.

The RPGM model and its variations present two major drawbacks. First, although the position of the reference point can be determined at all times, the position of nodes in a group is only known at each position update, requiring thus to adopt an extremely short update period Δt in order to guarantee up-to-date position information for all nodes. Second, explicit bounds on maximum linear and angular speed can only be imposed on the reference point; since the position of a node is randomly selected every Δt seconds within an area of radius d_{max} centered in the position of the group reference point, Δt and d_{max} must be carefully selected, in order to avoid violations on the linear and angular speed upper bounds of standard nodes.

The Reference Velocity Group Mobility (RVGM) model was proposed in [29] as an evolution of the RPGM model. In this model, nodes belonging to a same group share a reference speed vector, rather than a reference position. The authors in [29] propose the use of Gaussian variables for the generation of both reference speed vector and variations in speed and direction for each node in the group, with respect to the reference vector.

The RVGM model addresses one of the issues discussed for RPGM, since it provides a speed vector for each node, and allows to determine the position of each node at any time. However, in RVGM the spatial distribution of the nodes is heavily dependent on the initial position of the nodes. When nodes of a same group are close at network start, they maintain their physical proximity due to their similar speed vectors; oppositely, if nodes in a group are randomly positioned in the playground at start, no clear relation of their relative positions appears. If the playground is of infinite size, a relation will emerge in time, with each group moving in a different direction and forming a separate sub-network. In an area of limited size, this behavior will not emerge, as the limited playground will impose a finite maximum distance between nodes.

A common trait to the reference-based models discussed so far is the assumption of a persistent group binding between nodes. As a consequence, the performance of the models in scenarios characterized by dynamic group bindings is not assessed in existing literature.

3.2 Behavioral models

The concept of behavioral mobility modeling was introduced in [30]. In this approach the mobility pattern of a node is the result of a set of rules, that are mapped on corresponding forces applied to the node. Each force j generates an acceleration vector $\vec{a_j}$, and the combination of acceleration vectors leads to a global acceleration vector $\vec{a}$, that in turn determines the speed vector, and finally node mobility. The set of rules proposed in [30] determines the behavior of a node with respect to a) its desired destination, b) the surrounding environment, and c) the presence of other nodes. The main "desired destination" rule is the *Path Following* rule, that determines an acceleration vector towards a preset destination, taking into account the maximum speed allowed for the node. Rules taking into account the environment include *Wall Avoidance* and *Obstacle Avoidance*, that generate repulsive forces affecting the mobility pattern. Finally, rules that determine the behavior of a node in presence of other nodes include *Mutual Avoidance*, that avoids collisions between nodes, and the *Group Centering* and *Velocity Matching* rules, that force nodes to stay close in the space or speed domain, and can be considered as the behavioral equivalents to the RPGM and RVGM mobility models, respectively.

An extension of the behavioral model in [30] was recently proposed in [31], focusing on a more accurate modeling of the interaction with obstacles.

Behavioral mobility modeling was also investigated in [32], where a modular approach is proposed, in which basic rules are combined in order to generate complex behaviors such as group mobility. Basic rules include *Seek*, *Flee*, and *Arrive* for individual mobility, and *Pursuit*, *Evade* and *Interpose* for modeling the interaction between nodes.

Finally, a behavioral model based on a sociological analysis of the impact of social ties between individuals on mobility patterns was proposed in [33], again translating them in an acceleration vector.

Behavioral mobility modeling allows to introduce group mobility while maintaining information on the position of each node at any time, thus addressing the major issue affecting RPGM and most other reference-based group models. On the other hand, equations describing the rules governing the behavior of nodes include parameters that are

hard to relate with expected mobility patterns, as observed in [34]. Furthermore, behavioral models require the selection of normalizing and scaling factors to determine the relative weight of the different forces, making their adoption in modeling wireless networks extremely difficult.

4 THE MOMO MODEL

The MoMo model aims at the creation of a mobility pattern for each node, that emerges from the natural combination of individual mobility with group bindings. The two key components are thus the individual mobility model that a node follows in absence of group bindings, and the group bindings themselves, as described below.

4.1 Individual mobility model

Since, as indicated in Section 2, memoryless models lead to unrealistic mobility patterns due to the sudden changes in speed and directions, they were deemed unsuitable for adoption in MoMo. Memory-based models, on the other hand, can all potentially be adopted, but among them the Boundless model emerges as the best option for individual mobility modeling, as justified below.

The Inertia model may provide a straightforward mechanism for introducing memory in the selection of the speed vector. However, in this model, when a v and θ are updated, there is no correlation with their previous values, still leading to unrealistic patterns characterized by abrupt turns and speed variations, that, furthermore, make it impossible to meet requirements on maximum linear and angular speeds.

The Gauss-Markov model promises smoother patterns when compared to Inertia, but still does not provide a straightforward way to meet constraints on maximum speed and rotation in the generation of a mobility pattern. The adoption of a Gaussian probability density function, in particular, may lead to unrealistic values for node speed.

The lack of control on the resulting mobility patterns made thus both Inertia and Gauss-Markov models unsuitable for modeling individual mobility in MoMo.

The Boundless model shares with the Gauss-Markov model the capability of reproducing realistic movement patterns. The model has, however, the advantage of allowing the introduction of strict limits on speed, acceleration and rotation speed of nodes, making it easier to achieve realistic mobility patterns that meet predefined upper bounds. The model provides a good compromise between accuracy and flexibility, and was thus selected to model individual node mobility in MoMo. Figure 3 shows an example of movement pattern obtained with the Boundless mobility model within an area of $200x200\,m^2$, with $T = 1\,s$, $\gamma_{max} = \pi/2\,rad/s$, $a_{max} = 5\,m/s^2$ and $v_{max} = 5\,m/s$.

4.2 Group bindings

The MoMo model inherits from the model in [14] the idea of defining binding conditions related to physical proximity between nodes. The binding condition between two nodes i and j in the same group, referred to as group mates, is defined as:

$$d_{ij} \leq D_c, \tag{4}$$

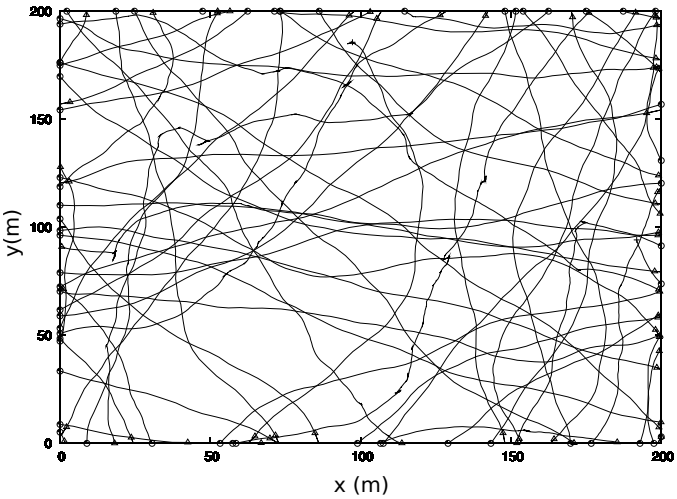

Fig. 3. Movement pattern of a node following the Boundless mobility model with $T = 0.1\,s$, $\gamma_{max} = \pi/2\,rad/s$, $a_{max} = 5\,m/s^2$ and $v_{max} = 5m/s$.

where $d_{ij} = d_{ji}$ is the distance between nodes i and j, and the distance D_c is a threshold in the model. If the binding condition in Eq. (4) is satisfied, the two nodes are said to be *connected*. Consider a group of size N. For the generic node j the set of N_j^c group mates that the node detects as connected is referred to as its *connected set*.

The ratio between N_j^c and the total number $N-1$ of group mates is referred to as grouping factor ρ_j:

$$\rho_j = \frac{N_j^c}{N-1}. \tag{5}$$

The behavior of node j depends on the following grouping condition defined on ρ_j:

$$\rho_j \geq \rho_{\min}, \tag{6}$$

where the grouping threshold $\rho_{\min}$ is another model parameter. Each node periodically checks whether the grouping condition is satisfied, with period Δu. Depending on the outcome, the node enters in either of the two following states:

- **Free**, when the grouping condition is satisfied. In this state the node moves freely according to the Boundless mobility model;
- **Forced**, when the grouping condition is not satisfied. In this state the node moves towards the closest group mate k not part of its connected set, in order to increase its grouping factor. v and θ are set as follows:

$$v = v_{max} \tag{7}$$

$$\theta = \begin{cases} \min\left(\beta_{kj}, \theta_{old} + \gamma_{max} T_{lu}\right), & \text{if } \beta_{kj} \geq \theta_{old} \\ \max\left(\beta_{kj}, \theta_{old} - \gamma_{max} T_{lu}\right), & \text{otherwise,} \end{cases} \tag{8}$$

where $\beta_{kj} = arctan\left(\frac{y_k - y_j}{x_k - x_j}\right)$, (x_k, y_k) and (x_j, y_j) are the positions of nodes k and j, respectively, θ_{old} is the previous direction, and T_{lu} is the time elapsed since the last position update[1]. Equations (7) and (8) ensure

1. In a discrete implementation of the model, with position updates every Δt, one has $T_{lu} = \Delta t$. Oppositely, if the position update is triggered by an on demand variable, T_{lu} measures the time elapsed from the last position update.

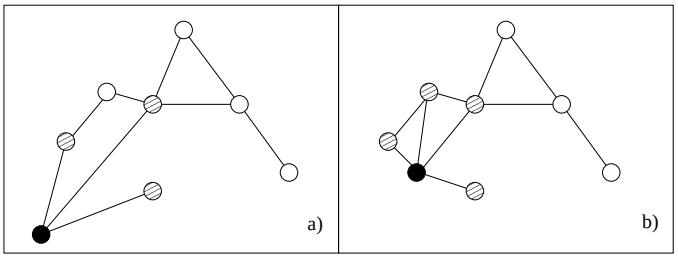

Fig. 4. Example of application of the MoMo mobility model for a group of 8 nodes, with $\rho_{min} = 0.5$. In a) the considered node (black node) is connected to 3 nodes (striped nodes) in its group, out of its 7 group mates, and the grouping factor $\rho = 3/7$ measured by the node is lower than the required ρ_{min}. As a consequence, the node enters in *Forced* mode and moves towards the closest group mate out of its connected set. The node maintains this behavior until the grouping condition is satisfied, evolving towards the situation in b), where the size of the connected set is increased to 4, corresponding to $\rho \geq \rho_{min}$.

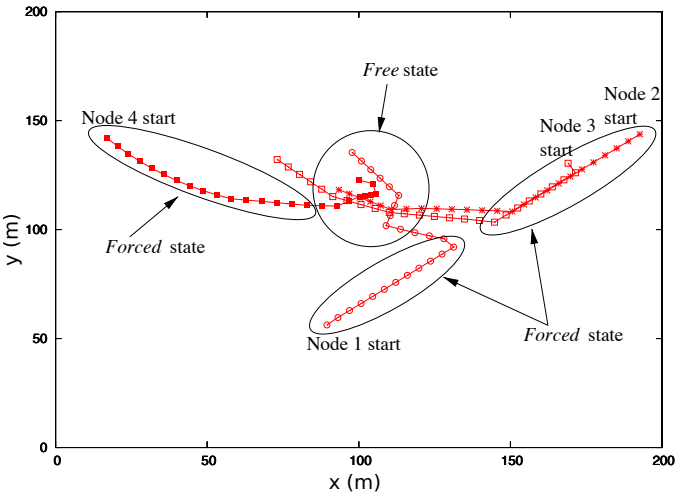

Fig. 5. Movement patterns obtained with the MoMo model for a group composed of 4 nodes with the following simulation settings: area size $200x200\,m^2$, maximum speed $v_{max} = 5\,m/s$, $a_{max} = 5\,m/(s^2)$, $\gamma_{max} = \pi/2\,rad/s$, $T = 5\,s$, $\rho_{min} = 0.7$, $D_c = 30\,m$, $\Delta u = 1\,s$. As nodes start from random positions, the grouping factor ρ is below the threshold for all of them. Nodes thus start moving in *Forced* state; as soon as one of them achieves $\rho > \rho_{min}$. it switches to *Free* state.

that node j reaches the selected group mate k in the shortest possible time frame, while avoiding, however, violations of constraints on linear and angular speed.

The behavior defined in the *Forced* mode, that is moving towards the closest group mate not in the connected set, is not the only possible one. More complex behaviors, e.g. moving towards the centroid of the positions of group mates, can be easily introduced in the framework of the MoMo model.

Figure 4 shows an example of application of the MoMo model in the case of a group of $N = 8$ nodes with $\rho_{min} = 0.5$. Lines between nodes indicate connectivity for the purpose of the MoMo mobility model. In Figure 4a) the size $N^c = 3$ of the connected set for the black node leads to a grouping factor $\rho = 0.43$. The grouping condition is thus not satisfied, and the node moves toward the closest group mate not part of its connected set, until the condition is satisfied (see the configuration shown in Figure 4b), in which $N^c = 4$, $\rho = 0.57$).

The definition of connectivity, and the corresponding meaning of the threshold D_c, is a key aspect in MoMo. The model allows for a flexible definition of the concept of being connected, depending on the application scenario:

- connectivity related to radio communications - in this case two nodes can be connected either through a direct radio link (physical layer connectivity), when they are within radio range, or through relaying, guaranteed by other group mates (network connectivity);
- connectivity based on a radio-independent parameter - for example, if a group corresponds to a security team, physical visibility may correspond to connectivity: a team member moves freely until it is able to see a minimum number of team members, and moves closer to the other members of the team when the condition is not met anymore.

An example of the movement pattern obtained with the MoMo model is presented in Figure 5.

5 Comparison Method

The comparison between mobility models is usually a complex problem due to the difficulty of defining objective comparison criteria. In the past, models were compared mainly by measuring their impact on network topology. This paper extends the analysis by defining, and using in the comparison, a set of intrinsic properties that a mobility model should possess:

- *accuracy* in modeling desired mobility patterns;
- *robustness* to variations in model parameter settings and consistency in generated mobility patterns;
- *flexibility*, allowing for the widest possible range of mobility scenarios to be addressed.

The first property, *accuracy*, refers to the capability of a mobility model of faithfully representing the desired mobility behavior, as defined by bounds on mobility model parameters. In this paper the accuracy of a model is assessed by measuring whether a model meets bounds on maximum linear speed and maximum rotation speed by means of two performance indicators: 1) the percentage of position updates violating the speed upper bound, and 2) the percentage of position updates violating the rotation speed upper bound.

Robustness takes into account the consistency of the mobility patterns generated by a model as a function of the variations in the model parameters settings. In order to assess the robustness of a model, the two performance indicators introduced above and the average speed of nodes are analyzed as a function of the position update period Δt and of the maximum threshold for the distance between two group mates, in models foreseeing such a threshold. It should be noted that models that define a speed vector for each node, such as RVGM and MoMo, allow to determine the position of nodes at any time, independently from Δt, by using Equation (1). Δt was, however, selected as one of the parameters to be considered in the analysis for two

reasons: a) some models, such as RPGM, do not provide a speed vector for each node, and position updates can be only provided every Δt seconds; b) most network simulators used in the performance evaluation of mobile wireless networks are actually discrete event simulators, favoring the implementation of mobility models as a sequence of periodic updates rather than as the evaluation of a time-continuous function. The latter reason, in particular, makes it very important to assess whether mobility models are robust with respect to variations of Δt.

Flexibility is defined as the capability to model dynamic scenarios where mobility characteristics change in time, leading to merging, splitting or disbanding of groups. Transitions between the two extreme cases of individual vs. tight group mobility, in particular, should be handled seamlessly by the mobility model, without generating unrealistic mobility patterns. The average speed of nodes in the network was measured while varying mobility characteristics, in order to detect any discontinuity or artifacts introduced by the model in generated patterns.

The assessment of the above properties is followed by the analysis of the *impact on topology* of wireless networks that, in turn, will affect the performance of network protocols, such as routing. The following performance indicators were adopted in this work to compare the mobility protocols in terms of their impact on network topology and connectivity [15], [16]:

- *Number of link changes*: number of transitions from *connected* to *disconnected* and viceversa, for links between nodes in the network. Its average over all the possible links in the network is the *average number of link changes*;
- *Link duration*: average duration of the link between two nodes, that is the average time that two nodes remain continuously within range. Its average over all the possible inks in the network is the *average link duration*;
- *Link availability*: percentage of total time during which a link between two given nodes is available, i.e. the two nodes are within transmission range. Its average over all the possible links in the network is the *average link availability*.

6 Performance analysis

6.1 Simulation settings

MoMo was compared against RPGM and RVGM group models in terms of accuracy, robustness and flexibility. The analysis of the impact on network topology was also extended to the Boundless and Gauss-Markov individual mobility models. Performance evaluation was carried out by computer simulation, using a simulator developed in the framework of the OMNeT++ simulation environment [35]. The simulation scenario was formed by a network of 16 nodes, divided into 4 groups of 4 nodes for group mobility. The simulation area size was $200x200\,m^2$, and each simulation run lasted 40000 seconds. The upper bounds on linear and angular speed to be met by models were set respectively to $v_{max} = 5\,m/s$ and $\gamma_{max} = \pi/2\,rad/s$. Model-specific settings adopted during simulations are presented in Table 1. In the case of RPGM and RVGM the following implementation choices were made, in order to ensure a fair comparison with MoMo:

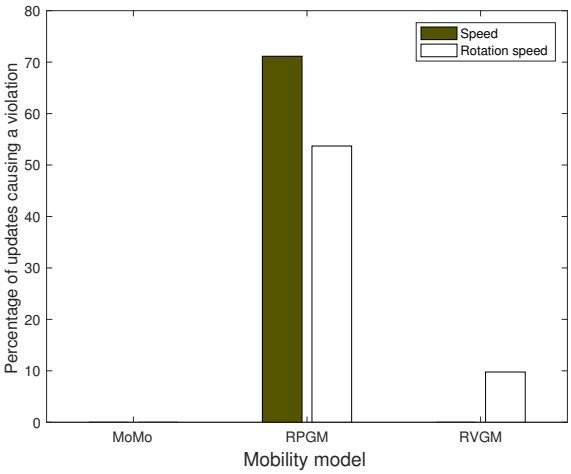

Fig. 6. Percentage of position updates violating the speed and rotation speed limits in the MoMo, RPGM and RVGM mobility models.

- *RPGM*: a group leader was selected in each group. The reference path for each group leader was generated using the Random Walk model in place of the Random Waypoint model originally proposed in [13], in order to avoid the side effects of the latter model, discussed in Section 2.
- *RVGM*: a group leader was selected in each group. The limits on minimum and maximum speed were enforced by adopting for both group leaders and standard nodes a truncated Gaussian distribution, rather than the Gaussian distribution originally proposed in [29].

In the analysis of the impact of models on network topology, a radio transmission range $d_{radio} = 30\,m$ was defined in order to determine if a link between two nodes is available. Independently of mobility patterns, nodes were always organized in groups from a communication point of view; each of the topology-related performance indicators introduced in Section 5 was thus separately measured for nodes belonging to the same communication group (*intra-group* values) and for nodes belonging to different groups (*inter-group* values). In the case of group mobility models, mobility groups were chosen to be the same as communication groups.

6.2 Accuracy, robustness and flexibility

6.2.1 Accuracy

Figure 6 shows the percentage of position updates violating the speed and rotation speed limits for MoMo, RPGM and RVGM, with the settings in Table 1. Figure 6 shows that both the MoMo and the RVGM are able to meet at all times the limit on linear speed, leading to no violations. The RPGM model, on the other hand, is unable to meet the bound on maximum speed, leading to a percentage of violations above 70%.

As for rotation speed, MoMo is again able to meet at all times the limit on upper rotation speed, with no recorded violations. This is not the case for RPGM and RVGM,

TABLE 1
Simulation settings for the considered mobility models

	Boundless	Gauss-Markov	MoMo	RPGM	RVGM
Δt	$1\,s$	$1\,s$	$1\,s$	$1\,s$	$1\,s$
T	$5\,s$	$5\,s$	$5\,s$	N/A	$5\,s$
v_{max}	$5\,m/s$	$5\,m/s$	$5\,m/s$	$5\,m/s$	$5\,m/s$
v_{min}	$0.001\,m/s$	$0.001\,m/s$	$0.001\,m/s$	$0.001\,m/s$	$0.001\,m/s$
a_{max}	$5\,m/(s^2)$	N/A	$5\,m/(s^2)$	N/A	N/A
γ_{max}	$\pi/2\,rad/s$	N/A	$\pi/2\,rad/s$	N/A	N/A
α	N/A	0.5	N/A	N/A	N/A
D_c	N/A	N/A	$30\,m$	N/A	N/A
ρ_{min}	N/A	N/A	0.5	N/A	N/A
Δu	N/A	N/A	$=\Delta t$	N/A	N/A
d_{max}	N/A	N/A	N/A	$30\,m$	N/A
σ_v	N/A	N/A	N/A	N/A	$1\,m/s$
σ_θ	N/A	N/A	N/A	N/A	$0.26\,rad$

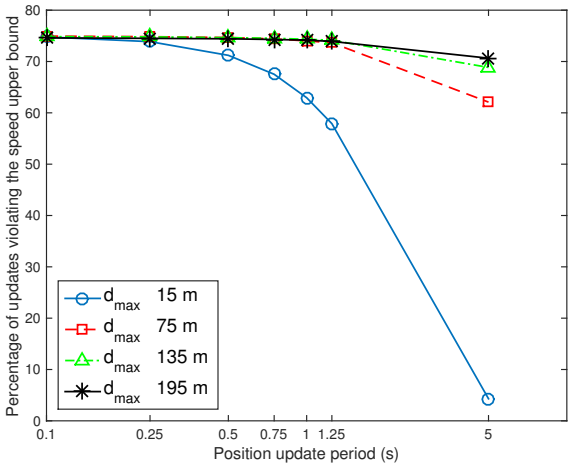

Fig. 7. Percentage of position updates violating the speed limit obtained with RPGM for four values of d_{max} as a function of the position update period Δt. All the remaining simulation settings were set according to Table 1.

leading to violations in 50% and 10% of position updates, respectively.

6.2.2 Robustness

For the robustness analysis, the maximum distance allowed between group members was determined by the D_c parameter for the MoMo model and by the d_{max} parameter for the RPGM model. In the case of the RVGM model no maximum distance is defined between group members, and as a consequence only the impact of Δt was investigated.

The structure of MoMo ensures that the upper bound on speed is always met: as a consequence, the percentage of updates violating the bound is zero for all values of Δt and D_c. The same is true for RVGM thanks to the adoption of a truncated Gaussian distribution for the absolute value of speed. This is not the case for RPGM, as shown in Figure 7, presenting the percentage of position updates leading to speed violations as a function of the position update time Δt, for different values of d_{max}. Results clearly highlight that the RPGM model fails to meet the upper bound on node speed. For low values of Δt, in particular, nodes that are not group leaders (that is 75% of the total number of nodes) almost never meet the bound on maximum speed, leading to an overall 75% of violations all over the network. The behavior of RPGM is directly related to the way positions of standard nodes are determined. In the case of small Δt values the position of nodes is updated very often; since at every position update positions of standard nodes are randomly generated within d_{max} meters of group leader position, a small Δt leads to a high probability of violating the speed upper bound. The longest distance a standard node can cover in RPGM at each update is in fact equal to:

$$d = 2d_{max} + v_{leader}\Delta t, \tag{9}$$

where v_{leader} is the current speed of the group leader. The corresponding maximum speed, for low values of Δt, can be approximated by:

$$v = \frac{d}{\Delta t} = 2\frac{d_{max}}{\Delta t} + v_{leader} \cong 2\frac{d_{max}}{\Delta t}. \tag{10}$$

For example, when $d_{max} = 10\,m$ and $\Delta t = 0.1\,s$, one has $v \leq 200\,m/s$, independently of the maximum speed allowed for group leaders.

Figure 7 highlights that the adoption of a large Δt mitigates the issue; this result comes, however, at the price of a lower accuracy in mobility modeling. Note in fact that in RPGM the position of standard nodes is only known at position update epochs, and cannot be derived according to eq. (1), since no speed vector is defined for standard nodes.

A similar trend can be observed for the upper bound on rotation speed. In this case as well the MoMo model always meets the bound and shows no violations independently of D_c and Δt. Figures 8 and 9 present the percentage of rotation speed violations for RPGM and RVGM, respectively. Both RPGM and RVGM adopt, in the generation of the reference path, a mobility model that does not allow to define a limit on rotation speed. As a consequence, compliance to the upper bound cannot be guaranteed even for the group leaders. Note that for both RVGM and RPGM the number of violations drops eventually to zero when Δt is large enough to allow a full rotation between two updates without causing a rotation speed violation, as shown in Figures 8 and 9 for $\Delta t = 5\,s$.

In the case of RVGM, the percentage of violations increases

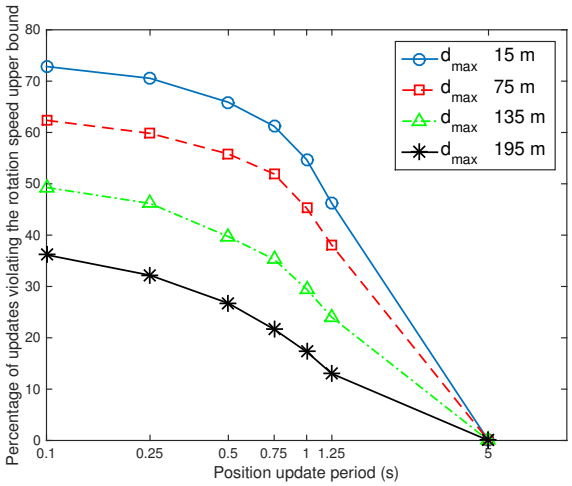
Percentage of updates violating the rotation speed upper bound
Position update period (s)
d_max 15 m
d_max 75 m
d_max 135 m
d_max 195 m

Fig. 8. Percentage of position updates violating the rotation speed limit obtained with the RPGM mobility model for four values of D_c as a function of the position update period Δt. All the remaining simulation settings were set according to Table 1.

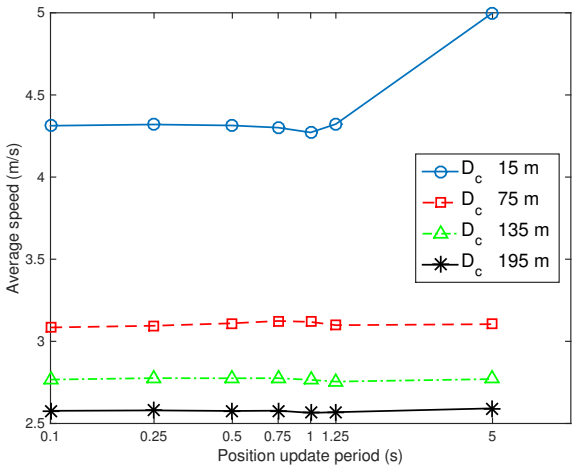

Fig. 10. Average speed obtained with the MoMo mobility model as a function of the position update time Δt for different values of D_c. All other simulations parameters were set as reported in Table 1.

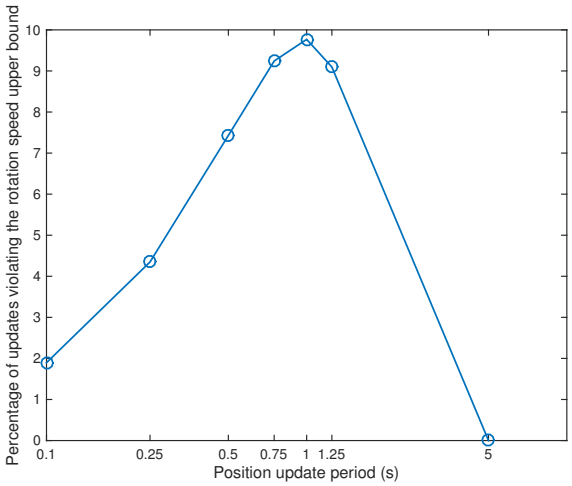

Fig. 9. Percentage of position updates violating the rotation speed limit obtained with the RVGM mobility model as a function of the position update period Δt. All the remaining simulation settings were set according to Table 1.

as Δt increases for small values of Δt, while the opposite trend is observed for higher values of Δt. This can be explained by observing that, as Δt increases, two opposite phenomena coexist:

1) the number of position updates decreases; since in RVGM rotation speed violations can only happen just after the selection of a new speed vector, the number of rotation violations is mainly depending on T, which is kept fixed in the simulations. As a consequence, although a detailed analysis of simulation results shows that the number of violations decreases with Δt, they become more relevant in percentage because the total number of position updates decreases at a faster rate;
2) the maximum rotation allowed for a node between two updates, given by $\gamma_{max} \cdot \Delta t$, increases, thus decreasing the probability for a direction update to cause a rotation speed violation.

For low Δt, phenomenon 1) prevails, leading to an overall increase in percentage of updates leading to a violation; as Δt increases beyond 1, phenomenon 2) becomes predominant and the percentage of updates decreases with Δt.
Figures 10, 11 and 12 show the average speed of nodes as a function of Δt for MoMo, RPGM and RVGM, respectively. MoMo shows a high robustness to variations of Δt; as one would expect, the average speed increases as D_c decreases, since a tighter group binding leads nodes to spend a larger amount of time in *Forced* mode, especially when node positions are not updated very often. This is shown in Figure 10 in the curve $D_c = 15\,m$ for $\Delta t = 5\,s$, where the average speed gets very close to the allowed maximum speed $v_{max} = 5\,m/s$.
Results for RPGM, presented in Figure 11, show that, for this model, the average speed strongly depends on Δt, due to the effect described by equation (10): in particular, the average speed is extremely unrealistic for low Δt that is, incidentally, the setting required for modeling the mobility of standard nodes with high accuracy.
Finally, RVGM shows very good robustness to variations of Δt, since the speed selection process is not influenced by the update period (see Figure 12).

6.2.3 *Flexibility*

The flexibility of mobility models was evaluated by randomly switching from group to individual mobility and viceversa. The switch between group and individual mobility for the three models was implemented as follows:

- in MoMo, ρ_{min} was set to zero, allowing all nodes to move in *Free* mode;
- in RPGM and RVGM all nodes were considered as group leaders, and thus moved independently of other nodes in the network.

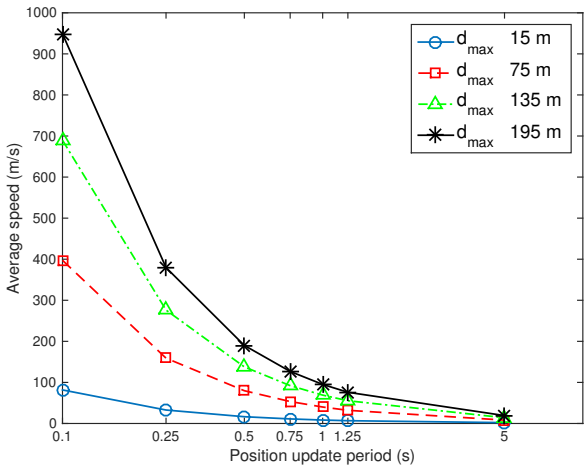

Fig. 11. Average speed observed in the RPGM mobility model as a function of the position update time Δt for different values of d_{max}. All remaining settings were as of Table 1.

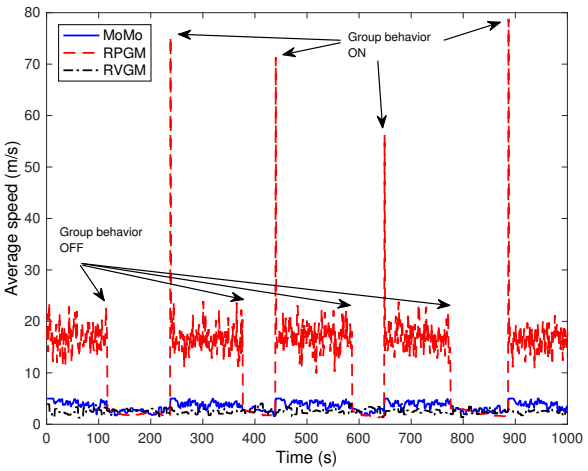

Fig. 13. Average speed obtained with the MoMo, RPGM and RVGM mobility models as a function of time. Group behavior was switched on and off during the observation, with average duration of on/off period equal to 100 s. All remaining settings were as of Table 1.

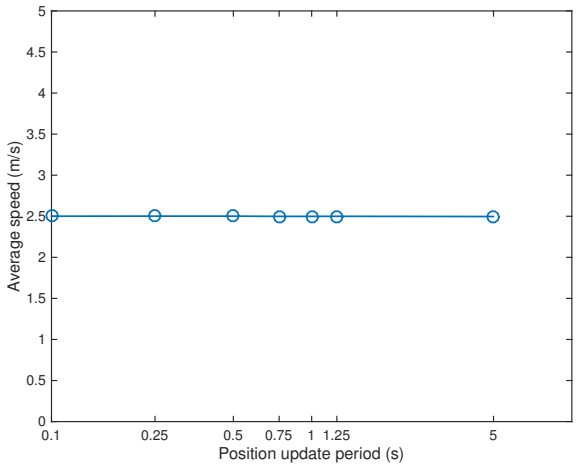

Fig. 12. Average speed obtained with the RVGM mobility model as a function of the position update time Δt. All remaining settings were as of Table 1.

Figure 13 shows the average speed as a function of time for MoMo, RPGM, and RVGM, in a simulation run under these settings. Results highlight the lack of flexibility of the RPGM model: the average speed for this model presents high spikes when nodes switch back to group mobility, due to the abrupt displacement of standard nodes from their previous position to a random position, within d_{max} meters from their group leader.

MoMo, on the other hand, does not show any anomalous behavior during transitions. Following a transition from individual to group mobility, in particular, nodes check the grouping condition and, if required, switch from *Free* to *Forced* mode and update their speed vector accordingly, without any discontinuity in their position. Figure 13 shows that the RVGM model suffers no discontinuities in average speed on transitions as well, again thanks to the adoption of a truncated Gaussian distribution.

Figure 14 extends the analysis by presenting both the average distance between nodes in the same group, and the average distance between all nodes as a function of time for the three models. The results highlight a strong difference of RPGM and MoMo vs. RVGM. RVGM is in fact unable to preserve proximity bindings between group mates, in particular after long periods of individual mobility. During these periods, nodes belonging to the same group spread across the simulation area, since their speeds and directions are independent. As a consequence, RVGM is only suitable for very specific mobility scenarios, where group members are not required to meet any bound on intra-group average distance. Figure 14 shows indeed that RVGM does not lead to different intra-group vs. inter-group average distance, while MoMo and RPGM lead to a significantly shorter intra-group distance.

Results highlight that MoMo is capable of combining the desirable properties of the RPGM and RVGM models, that is physical proximity between group mates (RPGM), and high robustness to variation of model parameters and mobility scenarios (RVGM).

6.3 Impact of mobility models on network topology

6.3.1 *Average number of link changes*

Figure 15 shows the average number of link changes per minute for all the considered mobility models, and for both inter-group and intra-group links.

As expected, results for individual mobility models do not present significant differences of intra-group vs. inter-group statistics, coherently with the absence of group relationship between nodes.

Moving to group models, MoMo causes a very high number of changes in links between nodes belonging to the same group; this is due to the choice of setting $D_c = d_{radio}$. Nodes can in fact move freely until they get out of radio connectivity, thus causing frequent intra-group link changes. The average number of inter-group link changes is, however,

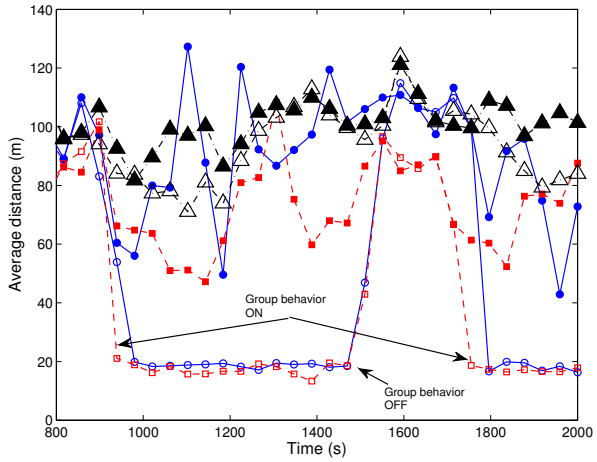

Fig. 14. Average distance obtained with the MoMo, RPGM and RVGM mobility models as a function of time. Group behavior was alternatively switched on and off with average duration of each period equal to 100 s. All remaining settings were the same as reported in Table 1 (MoMo: circles, RPGM: squares, RVGM: triangles. Empty markers: intra-group average distance; filled markers: network-wide average distance).

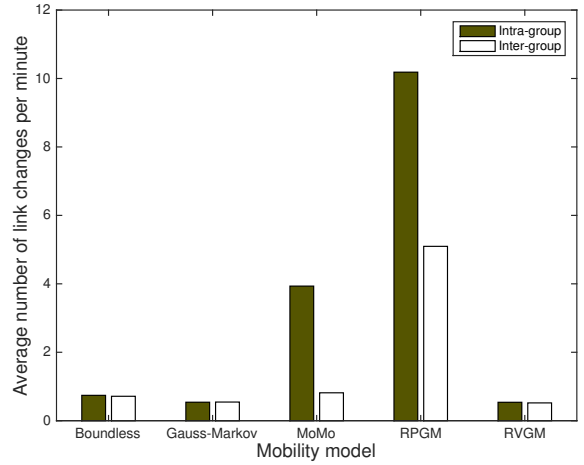

Fig. 15. Average number of link changes per minute for individual vs. group mobility models.

comparable with the one observed in individual mobility models. RPGM shares with MoMo the high number of changes in intra-group links, due to the setting $d_{max} = d_{radio}$. RPGM, on the other hand, leads to a high number of inter-group link changes as well. This discrepancy is an artifact, caused in RPGM by the abrupt position change of nodes that are not group leaders.

Moving to the RVGM model, no clear difference between intra-group and inter-group statistics can be observed. This result can be explained by reminding that the simulation area was of limited size, and thus prevented the groups from separating enough to achieve network partition. In a very large simulation area (theoretically of infinite size) groups would drift in different directions according to the speed vector of group leaders, and inter-group links would eventually disappear.

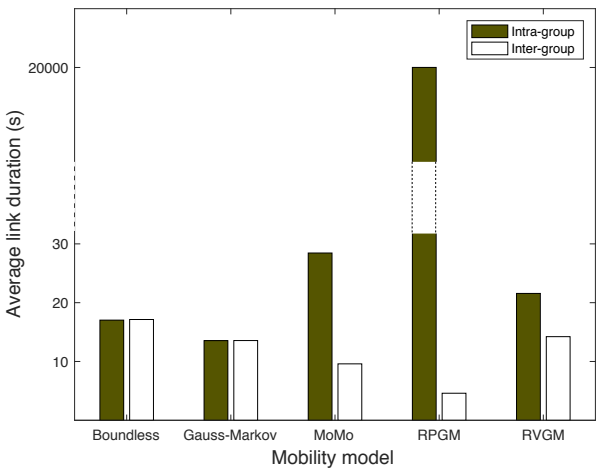

Fig. 16. Average link duration for individual vs. group mobility models. The y axis is adjusted in order to include the value of average intra-group link duration for RPGM.

6.3.2 *Average link duration*

Figure 16 shows the average link duration for all investigated mobility models and for both inter-group and intra-group links.

This metric very clearly tells apart group mobility models from individual ones. Group models lead to a significant difference in average link duration between intra- and inter-group links. In the case of RVGM, the higher duration for intra-group links derives from the circumstance that, if two nodes form an intra-group link, they have a high probability of keeping the link active, since they are characterized by similar speed and direction. In the case of MoMo and RPGM, physical proximity makes intra-group links more stable: nodes forming an intra-group link are in fact likely to remain close in the next future. Results in Figure 16 for the MoMo model show an average intra-group link duration that is larger than, but still still comparable to, the inter-group one, due to the decision of setting $D_c = d_{radio}$. The MoMo model allows, however, to model a wide range of mobility scenarios by properly setting D_c and ρ_{min}, as will be shown in Section 6.4.

Results for the RPGM model show that this model by far leads to the highest intra-group average link duration, with a value roughly equal to half of the simulation time. This result is heavily influenced by the fact that in the considered scenario ($d_{max} = d_{radio}$) links between standard nodes and group leader, accounting for half of the total number of intra-group links, are always guaranteed. Intra-group links between standard nodes, on the other hand, have a much shorter duration, since at each position update such nodes can fall out of radio connectivity while still meeting their proximity bound with the group leader. Average link duration between standard nodes was comparable to the duration for inter-group links, which was the lowest among all mobility models, as shown in Figure 16. Figure 16 also shows that, as expected, individual mobility models lead

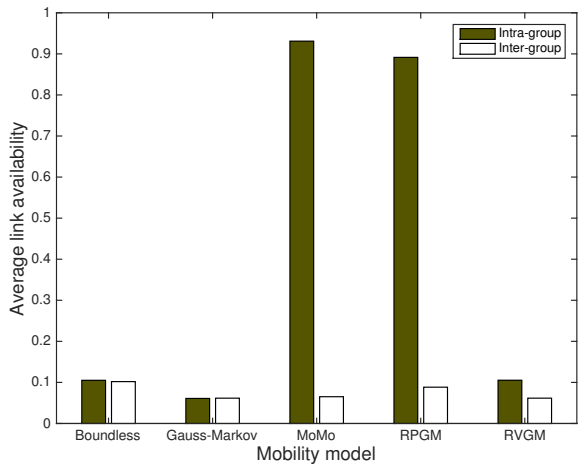

Fig. 17. Average link availability for different mobility models. All simulations were carried out with settings reported in Table 1.

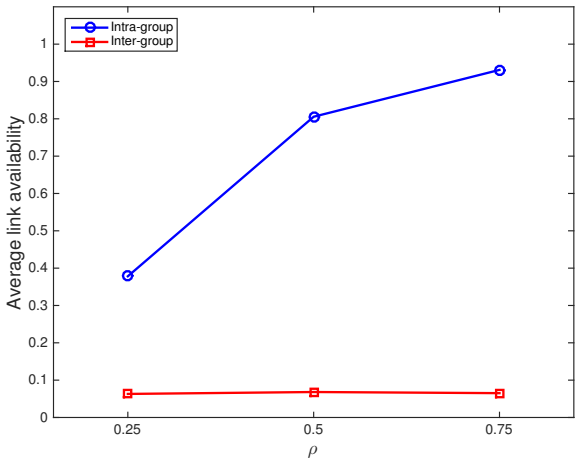

Fig. 18. Average link availability as a function of ρ in the MoMo model.

to no significant difference between intra-group and inter-group statistics.

Average link duration is an indirect indicator of the routing overhead due to connection maintenance; if group mobility is taken into account in route selection, by favoring intra-group routes, route maintenance requires a low overhead, since links within a group then last longer than inter-group links. This indicator is however incomplete, because it does not include the impact of the frequency with which a link switches from available to not available. This information is measured by the average link availability, analyzed in the next subsection.

6.3.3 *Average link availability*

Figure 17 shows the average link availability. Group vs. individual mobility models show a very different behavior in terms of link availability. Individual mobility models do not distinguish between intra- and inter-group links, and the average link availability is quite low, since links are between nodes that move in an independent fashion.

Group mobility models, on the opposite, highly privilege intra-group over the inter-group links. The similarity in the speed vector in RVGM, the physical proximity requirement of RPGM, and the group connectivity constraint of MoMo, all result in a higher availability of intra-group links; on the other hand, nodes from different groups are characterized by different movement patterns, resulting in less frequent links.

It is interesting to note that the approach adopted in MoMo mainly affects intra-group statistics, without dramatically impacting the statistics related to inter-group links, as can be observed by comparing the results of the Boundless model vs. MoMo.

Figure 17 also shows that, despite the very high average link duration previously observed for the RPGM model, the average link availability for RPGM is lower than for MoMo, due to the high instability in intra-group links between standard nodes.

6.4 Tuning the MoMo model

The grouping threshold ρ_{min} and the distance threshold D_c determine the characteristics of the mobility patterns generated by MoMo, and can be used to tune the model.

Figure 18 shows the average link availability measured as a function of the grouping threshold ρ_{min}; all other simulation settings were set as in Table 1.

A change in ρ_{min} is perceived when, in turn, it changes the minimum size N_f of the connected set required to keep a node in the *Free* state. The three values of ρ_{min} considered in Figure 18 correspond to the three possible values $N_f = 1$, 2, and 3, that can be imposed in a network of nodes forming groups of 4 units. The case $N_f = 0$ is not considered here, since in this case MoMo falls back to the Boundless model used in the *Free* state.

Results shown in Figure 18 highlight that the behavior of the model scales graciously with ρ_{min}: the intra-group links availability increases as ρ_{min} increases. This is coherent with the fact that an increase in N_f will lead to a more pronounced grouping behavior, and thus to a higher percentage of intra-group links being available. Results also show that variations of ρ_{min} do not significantly affect inter-group link availability.

The distance threshold D_c determines how tight the proximity binding is: a low D_c in fact forces the nodes to stay very close. Figure 19 presents the average link availability as a function of D_c. Results were obtained with $D_c = 10$, 30 and $50\,m$, while keeping all the other parameters as in Table 1. Figure 19 shows that for a high D_c, that relaxes the grouping requirement and allow nodes to move further from their group mates, the gap between inter-group and intra-group statistics is lower than with $D_c = 30\,m$ (see Figure 17). Oppositely, a low D_c introduces tight limits to the node movement patterns, leading the nodes to spend most of the time in *Forced* state, and resulting in an average link availability for intra-group links approaching unity, since $D_c < d_{radio}$.

Finally, Figure 20 shows the average link duration as a

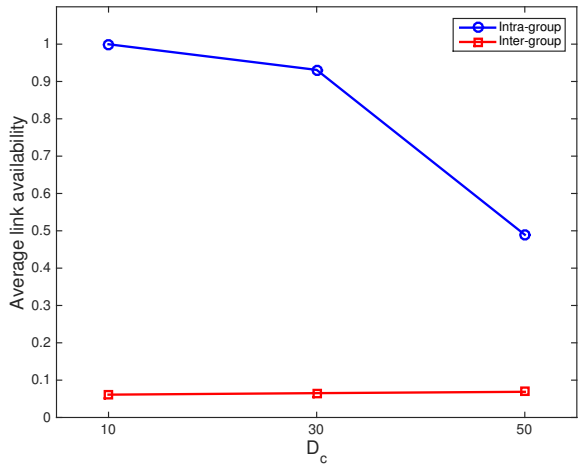

Fig. 19. Average link availability as a function of D_c in the MoMo model.

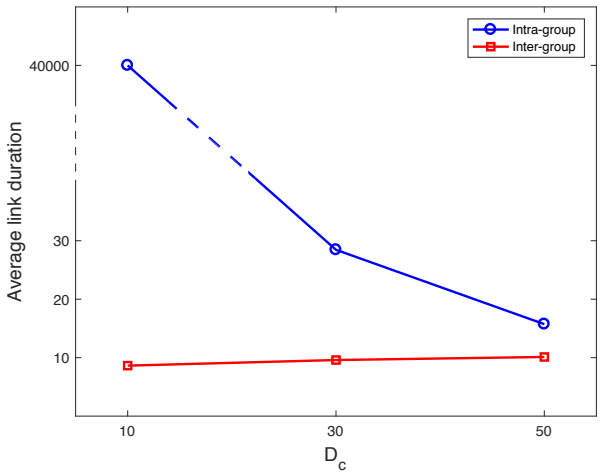

Fig. 20. Average link duration as a function of D_c in the MoMo model; the y axis was adjusted in order to include the value of average intra-group link duration for $D_c = 10$.

function of D_c, and further confirms that the behavior of MoMo can be reliably and effectively governed by varying the values of its parameters, covering all scenarios from tight group mobility to individual mobility.

In the above analysis the grouping condition check period, Δu, was always kept at its minimum value, equal to Δt. As a matter of fact, Δu may provide and additional degree of freedom in the tuning of MoMo: when $\Delta u > \Delta t$, nodes check less frequently if the grouping condition is satisfied, and thus spend more time in *Free* mode, leading to a stronger influence of the underlying Boundless mobility model on generated mobility patterns.

7 Conclusion

A new mobility model, referred to as MoMo, was proposed. MoMo is designed to accurately describe both individual movement of single nodes and group mobility emerging from interaction between nodes, aiming at modeling mobility in short distance wireless connectivity scenarios foreseeing dynamic group mobility, that will characterize 5G networks.

A set of intrinsic properties that mobility models should exhibit, in order to ensure a reliable generation of mobility patterns, was proposed. Performance indicators to analyze models in terms of such properties were also defined. The MoMo model was compared against existing standard and group mobility models, by means of computer simulation.

Results highlight that the MoMo model overcomes the limitations of preexisting group mobility models. MoMo guarantees the possibility of determining at any time the position of each node in the network and can flexibly and dynamically describe mobility patterns, ranging from loose or no group mobility to tight group mobility. MoMo is therefore a suitable candidate for modeling group and individual mobility in future network scenarios, and in particular in short distance wireless network scenarios that will characterize 5G systems.

Future work will address the analysis of spatial distribution of nodes as a result of the patterns generated by MoMo, and the use of captured mobility traces in 5G network scenarios in order to fine tune the MoMo model.

References

[1] H. Axelsson, P. Björkén, P. de Bruin, S. Eriksson, and H. Persson, "GSM/EDGE continued evolution," *Ericsson Review*, no. 1, pp. 20–29, 2006.

[2] P. Kela, M. Costa, J. Salmi, K. Leppanen, J. Turkka, T. Hiltunen, and M. Hronec, "A Novel Radio Frame Structure for 5G Dense Outdoor Radio Access Networks," in *IEEE 81st Vehicular Technology Conference (VTC-Spring)*, May 2015, pp. 1–6.

[3] "5G: a technology vision," Available at http://www.huawei.com/5gwhitepaper/, 2013.

[4] T. L. Marzetta, G. Caire, M. Debbah, I. Chih-Lin, and S. K. Mohammed, "Special issue on Massive MIMO," *Journal of Communications and Networks*, vol. 15, no. 4, pp. 333–337, August 2013.

[5] P. Kela, M. Costa, J. Turkka, M. Kolvisto, J. Wemer, A. Hakkarainen, M. Valkama, R. Jantti, and K. Leppanen, "Location Based Beamforming in 5G Ultra-Dense Networks," in *IEEE 84th Vehicular Technology Conference (VTC-Fall)*, September 2016, pp. 1–7.

[6] "Device-to-Device Communication in LTE-Advanced Networks: A Survey," *IEEE Communications Surveys and Tutorials*, vol. 17, no. 4, pp. 1923–1940, 2015.

[7] X. Ge, J. Ye, Y. Yang, and Q. Li, "User Mobility Evaluation for 5G Small Cell Networks Based on Individual Mobility Model," *IEEE Journal on Selected Areas in Communications*, vol. 34, no. 3, pp. 528–541, March 2016.

[8] IEEE 802.15.4 SG4a, "802.15.4IGa Informal Call for Application Response," July 2003. [Online]. Available: http://grouper.ieee.org/groups/802/15/pub/2003/15-03-0436-00-004a-echelo

[9] O. Safety and H. Administration, "Osha 29 cfr 1910.134(g)(4)(i) procedures for interior structural firefighting," Available on line at https://www.osha.gov/.

[10] T. L. E. E. A. Association, "Texas Law Enforcement Explorer Competition Training Guide," Available at http://www.ecsoexplorers.com/files/69934262.pdf, 2012.

[11] T. Camp, J. Boleng, and V. Davies, "A Survey of Mobility Models for Ad Hoc Network Research," *Wireless Communications and Mobile Computing (WCMC): Special issue on Mobile Ad Hoc Networking: Research, Trends and Applications*, vol. 2, no. 5, pp. 483–502, August 2002.

[12] J. Treurniet, "A Taxonomy and Survey of Microscopic Mobility Models from the Mobile Networking Domain," *ACM Computing Surveys*, vol. 47, no. 1, pp. 14:1–14–32, June 2014.

[13] X. Hong, M. Gerla, G. Pei, and C. C. Chiang, "A Group Mobility Model for Ad Hoc Wireless Networks," in *ACM International Workshop on Modeling and Simulation of Wireless and Mobile Systems (MSWiM)*, 1999, pp. 53–60.
[14] L. De Nardis, D. Domenicali, and M.-G. Di Benedetto, "Mobility model for Body Area Networks of soccer players," in *European Wireless Technology Conference (EuWiT)*, September 2010, pp. 65–68.
[15] F. Bai, N. Sadagopan, and A. Helmy, "IMPORTANT: A framework to systematically analyze the Impact of Mobility on PerfOrmance of RouTing protocols for Adhoc NeTworks," in *22nd Annual Joint Conference of the IEEE Computer and Communications Societies (INFOCOM 2003)*, vol. 2, March/April 2003, pp. 825–835.
[16] L. De Nardis, M. G. Di Benedetto, and S. Falco, "Higher layer issues, Ad-Hoc and Sensor Networks," in *UWB Communications Systems - A Comprehensive Overview*. Hindawi Publishing Corporation, 2006, ch. 4, pp. 205–252.
[17] M. Zonoozi and P. Dassanayake, "User mobility modeling and characterization of mobility pattern," *IEEE Journal on Selected Areas in Communications*, vol. 15, no. 7, pp. 1239–1252, July 1997.
[18] Y.-C. Hu and D. Johnson, "Caching Strategies in On-Demand Routing Protocols for Wireless Ad Hoc Networks," in *ACM International Conference on Mobile Computing and Networking (MobiCom)*, August 2000, pp. 231–242.
[19] A. Bar-Noy, I. Kessler, and M. Sidi, "Mobile users: to update or not to update?" in *IEEE Conference on Computer Communications (INFOCOM)*, vol. 2, June 1994, pp. 570–576.
[20] Y. B. Ko and N. H. Vaidya, "Location aided routing in mobile ad hoc networks," in *ACM International Conference on Mobile Computing and Networking (Mobicom)*, October 1998, pp. 66–75.
[21] D. B. Johnson and D. A. Maltz, *Dynamic Source Routing in Ad hoc Wireless Networks*. Kluwer Academic Publishers, 1996, ch. 5, pp. 153–181.
[22] E. Royer, P. Melliar-Smith, and L. Moser, "An Analysis of the Optimum Node Density for Ad hoc Mobile Networks," in *IEEE International Conference on Communications (ICC)*, vol. 3, June 2001, pp. 857–861.
[23] S. Basagni, I. Chlamtac, and V. R. Syrotiuk, "Dynamic source routing for ad-hoc networks using the global positioning system," in *IEEE Wireless Communications and Networking Conference*, September 1999, pp. 301–305.
[24] B. Liang and Z. J. Haas, "Predictive distance-based mobility management for multidimensional PCS networks," *IEEE/ACM Transactions on Networking*, vol. 11, no. 5, pp. 718–732, June 2003.
[25] Z. Haas, "A new routing protocol for reconfigurable wireless networks," in *IEEE International Conference on Universal Personal Communications (ICUPC)*, October 1997, pp. 562–565.
[26] M. Bergamo, "System design specification for mobile multimedia wireless network (MMWN)," DARPA - project DAAB07-95-C-D156, Tech. Rep., 1996.
[27] M. Sanchez and P. Manzoni, "Anejos: A java based simulator for ad-hoc networks," *Future Generation Computer Systems*, vol. 17, no. 5, pp. 573–583, March 2001.
[28] K. Blakely and B. Lowekamp, "A Structured Group Mobility Model for the Simulation of Mobile Ad Hoc Networks," in *2nd International Workshop on Mobility management and wireless access protocols (MobiWac '04*, ACM, Ed., October 2004, pp. 111–118.
[29] K. H. Wang and B. Li, "Group Mobility and Partition Prediction in Wireless Ad-Hoc Networks," in *IEEE International Conference on Communications (ICC)*, vol. 2, April 2002, pp. 1017–1021.
[30] F. Legendre, V. Borrel, M. D. De Amorim, and S. Fdida, "Reconsidering microscopic mobility modeling for self-organizing networks," *IEEE Network*, vol. 20, no. 6, pp. 4–12, November-December 2006.
[31] R. Beuran, S. Miwa, and Y. Shinoda, "Behavioral Mobility Model with Geographic Constraints," in *27th International Conference on Advanced Information Networking and Applications Workshops*, March 2013, pp. 470–477.
[32] A. Medina, G. Gursun, P. Basu, and I. Matta, "On the Universal Generation of Mobility Models," Boston University, Tech. Rep. 2010-014, 2010.
[33] V. Borrel, F. Legendre, M. Dias de Amorim, and S. Fdida, "SIMPS: Using Sociology for Personal Mobility," *IEEE/ACM Transactions on Networking*, vol. 17, no. 3, pp. 831–842, June 2009.
[34] H. Tripp, R. Hancock, A. Medina, and P. Basu, "Obtaining Generic Mobility Models from Network Properties and Trace Data," in *2010 Annual Conference of the International Technology Alliance (ACITA'10)*, May 2010.
[35] A. Varga, "OMNeT++," *IEEE Network Interactive*, vol. 16, no. 4, July 2002.

Luca De Nardis (M'98) is an Assistant Professor with the DIET Department, Sapienza University of Rome. He received the Laurea and Ph.D. degrees from the Sapienza University of Rome, Italy, in 2001 and 2005, respectively. In 2007, he was a Post-Doctoral Fellow with the EECS Department, University of California at Berkeley, USA. He authored or co-authored over 100 publications in international peer-reviewed journals and conferences. His research interests focus on UWB radio technology, medium access control, routing and positioning protocols for wireless networks, and on the design of cognitive wireless networks.

Maria-Gabriella Di Benedetto obtained her Ph.D. degree in 1987 from Sapienza University of Rome, Italy. In 1991, she joined the Faculty of Engineering of Sapienza University of Rome, where she is a Full Professor of telecommunications. She has held visiting positions at the Massachusetts Institute of Technology, USA, the University of California, Berkeley, USA, and the University of Paris XI, France. In 1994, she received the Mac Kay Professorship award from the University of California, Berkeley. Her research interests include wireless communication systems, in particular impulse radio communications, and speech. She is an IEEE Fellow.